ACS APPLIED MATERIALS & INTERFACES

www.acsami.org

Research Article

Multi-material 3D Printing of Mechanochromic Double Network Hydrogels for On-Demand Patterning

Bo Xu, Hezhen Wang, Zixiong Luo, Jiping Yang, and Zhijian Wang*

Cite This: *ACS Appl. Mater. Interfaces* 2023, 15, 11122−11130

Read Online

ACCESS | Metrics & More | Article Recommendations | Supporting Information

ABSTRACT: Cephalopods can change their color and patterns by activating the skin chromatophores for camouflage. However, in the man-made soft material systems, it is greatly challenging to fabricate the color-change structure in the desired patterns and shapes. Herein, we employ a multi-material microgel direct ink writing (DIW) printing method to make mechanochromic double network hydrogels in arbitrary shapes. We prepare the microparticles by grinding the freeze-dried polyelectrolyte hydrogel and immobilize the microparticles in the precursor solution to produce the printing ink. The polyelectrolyte microgels contain mechanophores as the cross-linkers. We adjust the rheological and printing properties of the microgel ink by tailoring the grinding time of freeze-dried hydrogels and microgel concentration. The multi-material DIW 3D printing technique is utilized to fabricate various 3D hydrogel structures which could change into a colorful pattern in response to applied force. The microgel printing strategy shows great potential in the fabrication of the mechanochromic device with arbitrary patterns and shapes.

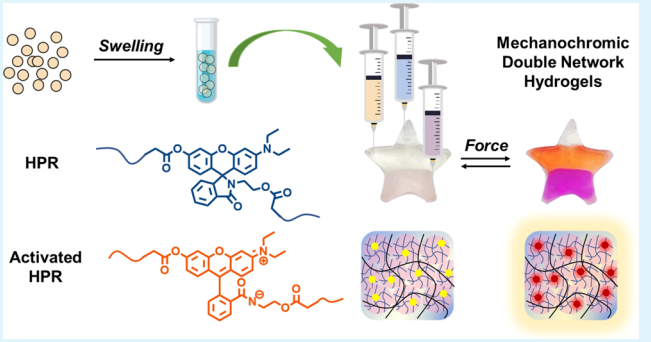

KEYWORDS: *3D printing, mechanochromism, double network hydrogels, rhodamine, multi-material printing*

1. INTRODUCTION

The cephalopods are capable of changing their body color patterns for camouflage and signaling displays, by activating the skin chromatophores in their bodies.[1] These skin chromatophores can be greatly deformed by contracting the attached radial muscles, generating colorful patterns. The color change is reversible, and the skin of cephalopods recovers to the initial state after releasing the muscles. Inspired by the cephalopods, several strategies have been developed to imitate the force-induced color change abilities in the man-made soft material systems, with the incorporation of the strain-dependent cracks and folds,[2] the liquid crystal elastomer masks,[3] bioluminescent unicellular marine algae,[4] microfluidic channels,[5] and so forth. These color-change systems are usually fabricated in multi-layer structures, which are complex and time-consuming. It is challenging to make the soft color-change systems in arbitrary shapes and patterns.

Recently, the mechanochromic materials, which can change their colors under the applied force, have drawn much attention. They could be produced by introducing the periodic structure,[6,7] the aggregation of dyes,[8,9] the incorporation of the mechanophores,[10−12] and so forth. Among them, the materials produced by incorporating the mechanophores are homogeneous, through the incorporation of the mechanophores in the polymer network, such as spiropyran,[13−16] rhodamine,[17−20] 1,2-dioxetane,[21−23] diarylbibenzofuranone,[24−26] Diels-Alder adducts,[27,28] and so forth. The mechanophores change their chemical structures and switch their optical properties in response to mechanical force. The development of mechanochromic materials has provided an alternative to realize the camouflage in the soft material systems. For example, Wang and co-workers fabricated an electro-mechanical responsive system with the mechanochromic elastomers to generate various fluorescent patterns.[29] The colorful patterns were produced by the wrinkling instability of the multi-layer structure containing soft and hard elastomers, under the application of voltage.

To build the soft color-change system in arbitrary shapes and patterns, three-dimensional (3D) printing, a kind of technique to fabricate objects by the computer-aided design, has been utilized. Boydston and co-workers incorporated the spiropyran derivative mechanophores into the main chain of polycaprolactone (PCL).[30] The mechanochromic PCLs were printed into different shapes with a commercial fused filament deposition manufacturing printer. Craig and co-workers

Received: December 15, 2022
Accepted: February 9, 2023
Published: February 20, 2023

ACS Publications

© 2023 American Chemical Society

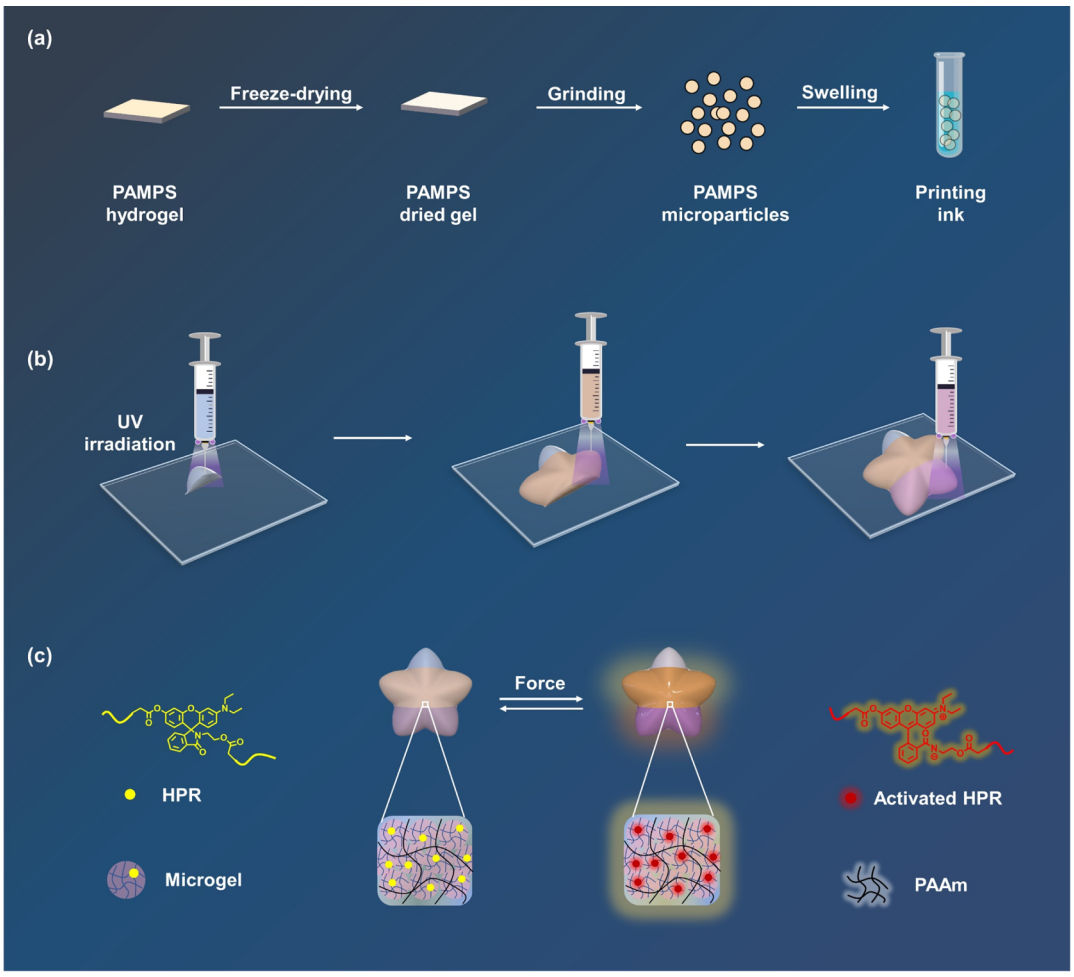

Figure 1. Schematic illustration of the (a) preparation steps of the microgel printing ink, (b) multi-material printing process of the microgel ink with different mechanophores, and (c) mechanism of the force-induced color change of the printed hydrogels.

explored a direct ink writing (DIW) printing strategy of viscous silicone ink which was made from spiropyran mechanophore-embedded polydimethylsiloxane (PDMS) beads.[31] The printed PDMS structure was further cured into highly cross-linked elastomers and showed a color change from white to purple under compression.

Compared with the PCL and PDMS, hydrogels are composed of a large amount of water and have low modulus and large stretchability. They have shown great potential in the biomedical device,[32−34] flexible electronics,[35−37] soft machines,[38−42] and so forth. For instance, the hydraulic hydrogel robot shows excellent optical and sonic camouflage ability in water.[43] With the covalent incorporation of the mechanophores, hydrogels could be capable of changing color under mechanical force.[19,20,44,45] However, the mechanochromic hydrogels are usually made as the double network hydrogels (DNHs), which are tough enough to trigger the activation of the mechanophores.[46] The mechanophores are covalently incorporated into the first polymer network of the hydrogels. Then, the first polymer network is further swollen in the polymerizable precursor solution, and the DNHs are obtained after further UV curing. The swelling and two-step polymerization processes make it greatly challenging to fabricate a mechanochromic hydrogel in arbitrary shapes and patterns.

In this work, we employ a multi-material microgel DIW printing method to fabricate the mechanochromic hydrogels in arbitrary shapes. The printing ink is composed of the microgels containing polymerizable monomers, which is prepared following similar procedures in the microgel printing methods.[47−50] We first prepare a polyelectrolyte network embedded with mechanophores inside. The polyelectrolyte hydrogel is freeze-dried and ground. Then, the obtained microparticles are swollen in a polymerizable acrylamide (AAm) solution to produce the printing ink. The AAm solution would form a polymer network under UV curing, connecting the polyelectrolyte microgels together. The cured hydrogels are strong and tough to trigger the activation of the mechanophores under applied external force. Furthermore, we are capable of printing different patterns by tailoring the composition of the microgel inks. The microgel printing technique provides an effective method to fabricate the mechanochromic hydrogels in arbitrary shapes and patterns.

2. RESULTS AND DISCUSSION

As shown in Figure 1a, we first prepare a polyelectrolyte network poly(2-acrylamido-2-methyl-1-propanesulfonic acid) (PAMPS) with ammonium persulfate (APS) as the thermal initiator, the hybrid phenol-rhodamine (HPR) mechanophore, and *N*,*N*′-methylene bisacrylamide (MBAA) as the cross-linker, following the procedures reported previously.[46] The concentrations of HPR, MBAA, and APS are the same as 2×10^{-2} mol/L, and the AMPS is added with a concentration of 1

https://doi.org/10.1021/acsami.2c22564
ACS Appl. Mater. Interfaces 2023, 15, 11122−11130

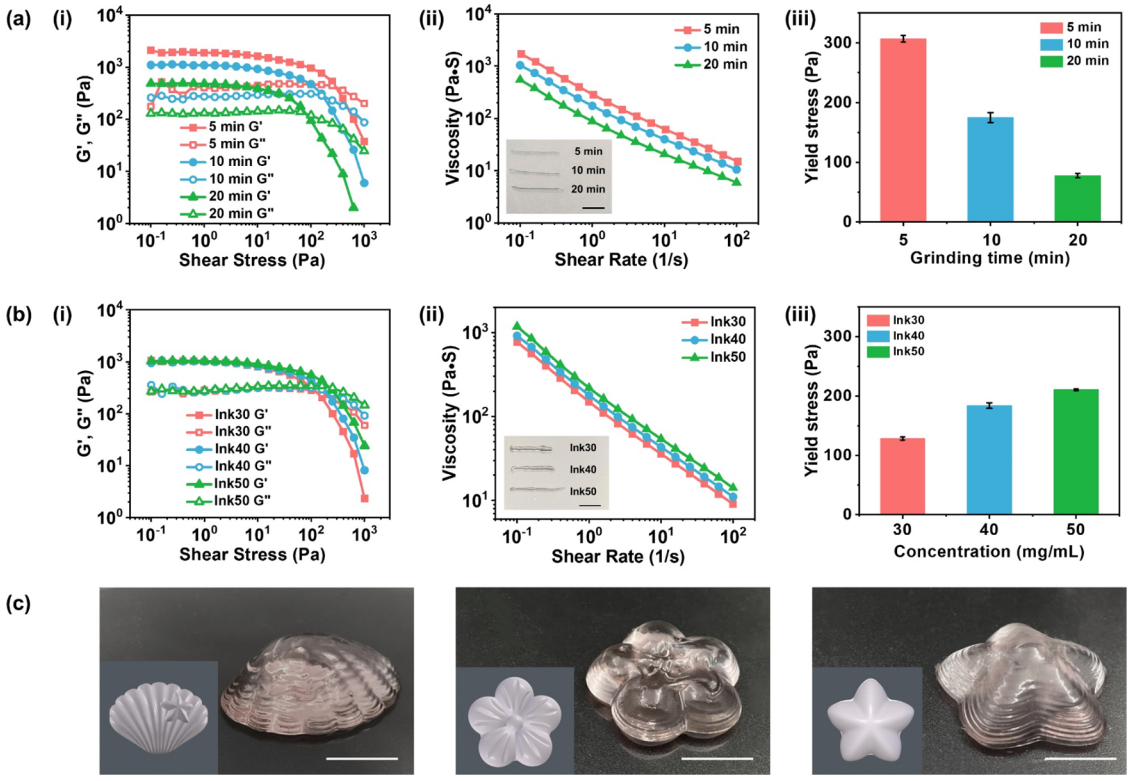

Figure 2. (a) Rheology properties of microgel inks made with different grinding times. (i) Shear storage modulus (G') and shear loss modulus (G'') as a function of shear stress. (ii) Viscosity as a function of shear rate. (iii) Plot of the yield stress versus grinding time. (b) Rheology properties of the microgel ink with different microgel concentrations: (i) shear storage modulus (G') and shear loss modulus (G'') as a function of shear stress. (ii) Viscosity as a function of shear rate. (iii) Yield stress. The insets are the 3D models of the printing shapes. Scale bars: 1 cm. (c) Photographs of the printed hydrogel structures: a hydrogel seashell, a hydrogel flower, and a hydrogel star.

mol/L. After curing in the oven with a temperature of 50 °C for 1 h, the obtained PAMPS hydrogel is immersed in the sodium hydroxide solution (1×10^{-2} mol/L). Then, the neutralized PAMPS hydrogel is freeze-dried and ground into microgel particles (Figure S1). The microparticles are a little reddish after grinding. The ground dried microparticle powders are swollen in the precursor solution of the second polymer network, which is prepared by dissolving monomer acrylamide, cross-linker MBAA, and photoinitiator I2959 in the solution of borax/sodium hydroxide buffer solution (pH = 10). The detailed procedures are described in the Experimental Section. The obtained microgel ink is colorless and transparent (Figure S2). The mechanochromic property of the printed hydrogels can be tailored by adjusting the kinds or concentrations of the mechanophores in the printing inks. Then, the prepared microgel ink is extruded by a commercial printer (Engineering SR, Hyrel) equipped with a UV LED light (365 nm) (Figure 1b). After being extruded out of a nozzle with a diameter of 0.52 mm, the printed structure is further cured under UV light (365 nm) for 15 min to form the second polymer network. It is convenient to print multiple microgel inks with or without mechanophores by switching the ink reservoir in the DIW printing technique. As shown in Figure 1b, we could print a star shape with three kinds of microgel inks which have different mechanochromic behaviors. After being stretched or compressed, the cured printed hydrogel structures would exhibit color change, which results from the transition from the spirolactam structure to the planarized zwitterionic form in the rhodamine mechanophores (Figure 1c).

To be successfully printed, the microgel ink should flow during extrusion and maintain the printed shape after deposition. We adjust the rheological property of the microgel ink by tailoring the microparticle size and the microgel concentration. The size of the ground microparticles highly depends on the grinding time of the freeze-dried PAMPS. As measured by the particle size analyzer (Mastersizer 3000), the microparticles obtained with a grinding time of 5, 10, and 20 min show a size below 150 μm, and the amount of microparticles with smaller size increases with the increase in grinding time (Figure S3). We immobilize the ground PAMPS microparticles in the precursor solution containing AAm, MBAA, and I2959 and study the rheological behavior of the microgel by the dynamic stress sweep and frequency sweep at room temperature. As shown in Figure 2a(i), all the microgel inks prepared with different microparticle sizes show a typical shear thinning behavior. At the low shear stress, the loss modulus (G'') is smaller than the storage modulus (G'), which means that the microgel ink acts in the solid-like state. As the shear stress increases to a high value, the loss modulus becomes larger than the storage modulus, indicating that with a larger shear stress, the ink becomes a fluid-like state. The viscosity of the microgel ink also shows a highly shear rate-dependent behavior, with a high viscosity at the low shear rate and a low viscosity at the high shear rate [Figure 2a(ii)]. The viscosity at the same shear rate becomes lower when the grinding time of the microparticles increases because of the smaller average microparticle size. The yield stress of the microgel ink, which is defined as the cross-point between the storage modulus and loss modulus, decreases with the increase

https://doi.org/10.1021/acsami.2c22564
ACS Appl. Mater. Interfaces 2023, 15, 11122−11130

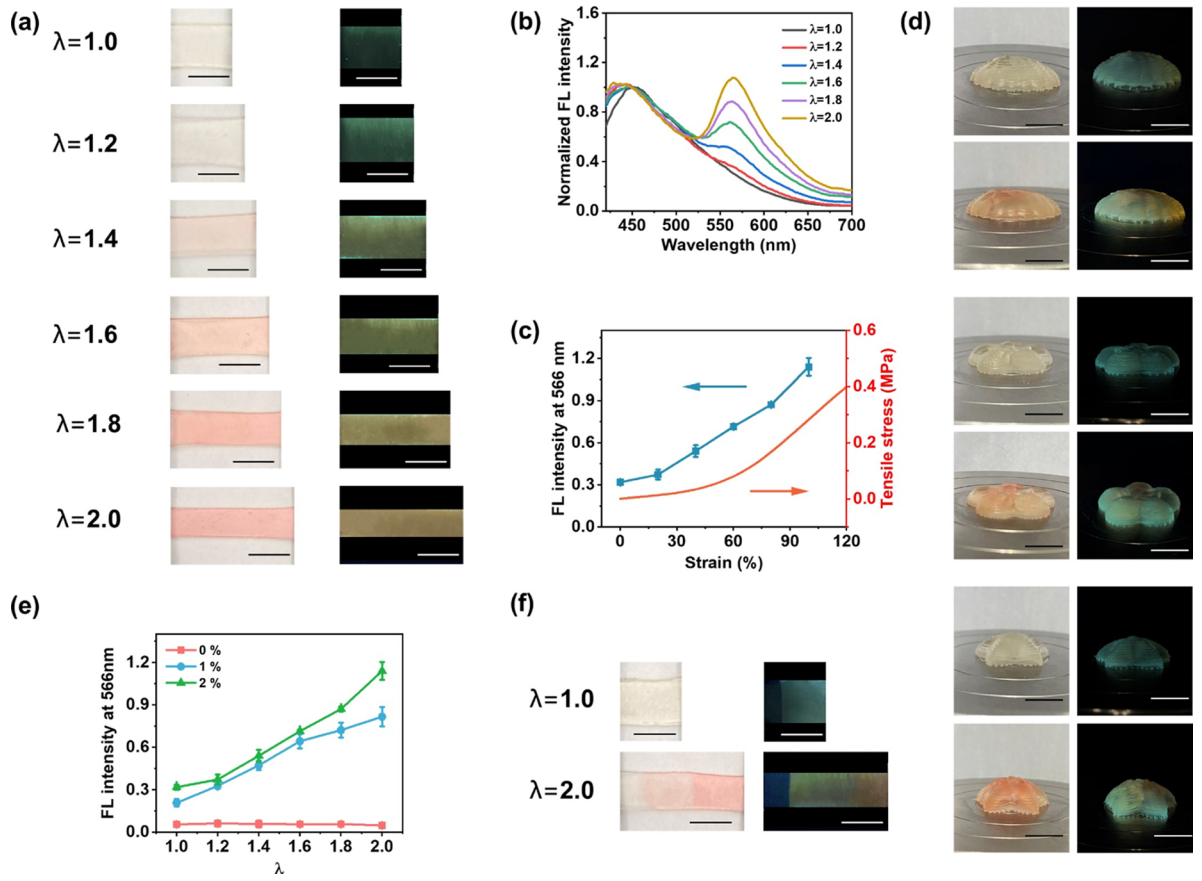

Figure 3. (a) Optical and fluorescent photographs of stretched rectangular-shaped DNHs with different stretches. Scale bars: 1 cm. (b) Fluorescence spectra of the DNHs with different stretches. (c) Plot of fluorescence intensity at a wavelength of 566 nm and the tensile stress versus the strain in the uniaxial tensile test. (d) Optical and fluorescent photographs of the hydrogel seashell, flower, and star after being compressed and released. Scale bars: 1 cm. (e) Plot of the fluorescence intensity at a wavelength of 566 nm versus stretch for the DNHs with different HPR concentrations. (f) Optical and fluorescent photographs of stretched DNHs printed with multiple materials in the stretch of 1.0 and 2.0. Scale bars: 1 cm.

in the grinding time [Figure 2a(iii)]. The microgel ink produced with a grinding time of 20 min has the lowest viscosity and yield stress. We further extrude the microgel inks from the nozzle. It is found that the filament printed by microgel ink with a grinding time of 20 min could not maintain its shape after extrusion [inset in Figure 2a(ii)]. Thus, in the following experiments, we use the microgel ink with the grinding time of the microparticles as 10 min for 3D printing.

We further study the influence of the microgel concentration on the rheology of the printing inks. The microgel ink is prepared with the microparticles with a grinding time of 10 min. The three kinds of microgel inks with a microgel concentration of 30, 40, and 50 mg/mL are used, which are termed Ink30, Ink40, and Ink50, respectively. All the three printing inks demonstrate typical shear thinning phenomena [Figure 2b(i)]. At low shear stress, G' is larger than G'', showing that the ink is in a solid-like state. With the increase in shear stress, when G'' exceeds G', the ink is transformed into a liquid-like state. Thus, the ink could be extruded through the needle and maintain its shape after being loaded on the substrate. The viscosity and yield stress of the inks also increase with the increase in the microgel concentration [Figure 2b(ii,iii)]. We extrude the three microgel inks on a glass substrate through the nozzle. The filament made with Ink30 and Ink40 would diffuse after extrusion and could not maintain its shape, while that made from Ink50 exhibits good appearance [inset in Figure 2b(ii)]. Therefore, in the following experiments, we use the microgel ink with a grinding time of 10 min, and the concentration of the microgels is set as 50 mg/mL. Three kinds of shapes, including the seashell, flower, and star, are printed as shown in Figure 2c. The printed structures have good shapes and resolutions, demonstrating excellent printing quality of the microgel ink.

The mechanical property of the printed hydrogel is measured by uniaxial tensile test (Figure S4). The printed hydrogel shows a tensile strength of 0.56 MPa and a strain at break of 153%. We uniaxially stretch the printed hydrogel and take photographs under the visible light (Figure 3a). The printed hydrogel turns reddish when the stretch reaches around 1.4, demonstrating that under such a stretch, the mechanical force is effectively transferred and triggers the activation of the HPR mechanophores. The HPR mechanophores transform into a zwitterionic structure with a longer absorption wavelength. As the stretch increases, the color of the hydrogel goes deeper, indicating the increase in the amounts of the activated HPR mechanophores. In addition, the stretched hydrogel exhibits a significant fluorescent color change. Under the illumination of 365 nm UV light, the as-prepared hydrogel shows a fluorescent green color. After stretching, the hydrogel gradually shifts to the fluorescent orange color. We measure the fluorescent spectra of the printed hydrogels to quantitatively study the activation of the

https://doi.org/10.1021/acsami.2c22564
ACS Appl. Mater. Interfaces 2023, 15, 11122−11130

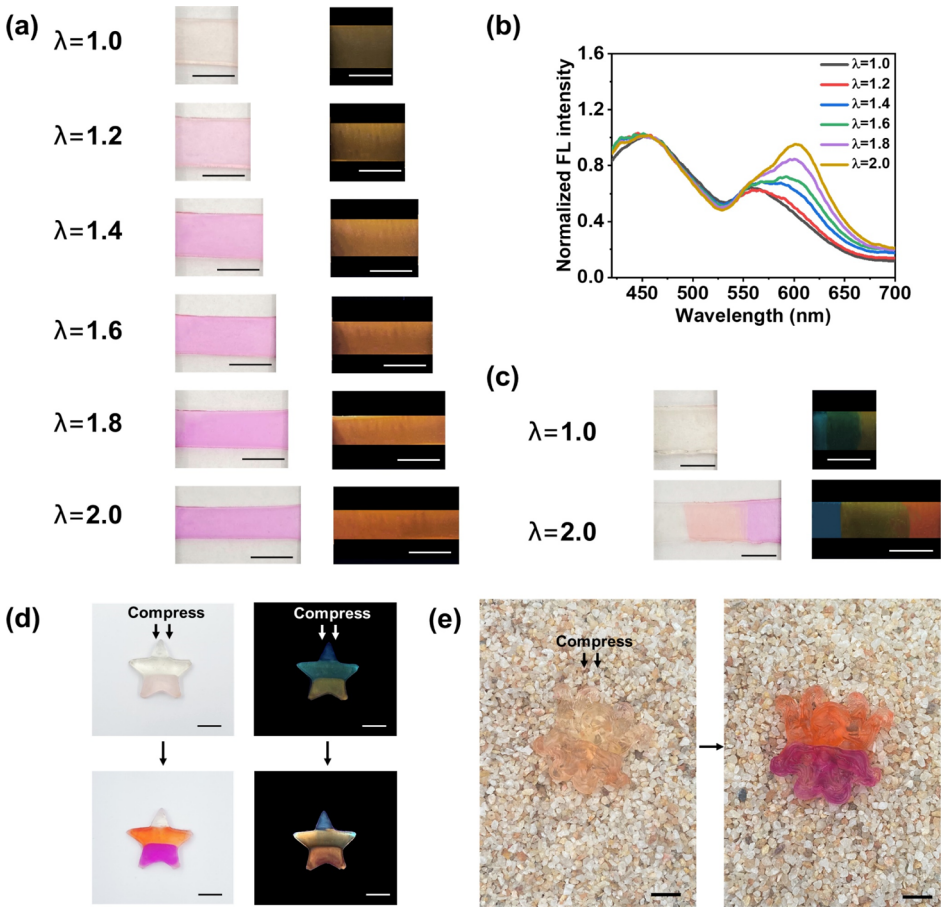

Figure 4. (a) Optical and fluorescent photographs of stretched rectangular-shaped DNHs with different stretches. Scale bars: 1 cm. (b) Fluorescence spectra of the TAR-embedded hydrogels with different stretches. (c) Optical and fluorescent photographs of DNHs printed by multiple microgel inks. The hydrogel shows significant color change under the stretch of 2.0. Scale bars: 1 cm. (d) Optical and fluorescent photographs of the hydrogel star before and after being compressed. Scale bars: 1 cm. (e) Optical photographs of the hydrogel octopus after being compressed. Scale bars: 1 cm.

HPR mechanophores during stretching (Figure 3b). The as-prepared hydrogel displays a fluorescent emission peak at 450 nm. As the stretch increases, the fluorescence intensity at 566 nm gradually increases, which corresponds to the opened spirolactam structure of the HPR mechanophores. The fluorescence intensity at 566 nm (I_{566}) versus stretch is plotted in Figure 3c. When the strain reaches 40%, the hydrogel shows a significant increase in the fluorescent intensity at 566 nm, while the stress is as low as 40 kPa. The hydrogel structure printed by microgel ink shows comparable mechanochromic sensitivity with that made from the swelling method.[46] The mechanochromic behaviors of the printed hydrogels are reversible. The fluorescent color of the stretched hydrogel would disappear after being relaxed under the ambient condition for 2 h (Figure S5). We further study the cyclic mechanochromic behaviors of the hydrogels by measuring the fluorescent spectra. The printed hydrogel is stretched to 2 and placed under ambient temperature for recovery. It is found that the I_{566} increases from 0.39 to 1.1 after stretching for the first time. After being relaxed for 2 h, the I_{566} recovers to 0.4. The I_{566} reaches 0.7 and 0.6 in the second and third cycle, respectively. The maximum fluorescent intensity at 566 nm decreases when increasing the cycling numbers. The I_{566} only reaches 0.4 in the seventh cycle (Figure S6). The color change in the printed hydrogels could be not observed. It is because that the PAMPS microgel network would be broken during the cyclic deformation. The efficiency for transferring the mechanical force would decrease in the broken network. The phenomenon is also found in the previous report.[46] The printed mechanochromic hydrogel structures are also sensitive to the compressive stress (Figure 3d). The printed 3D structures, including seashell, flower, and starfish, are compressed. The hydrogel structures change from colorless to red, observed by naked eyes. Under the irradiation of 365 nm UV light, the fluorescent color clearly changes from green to orange. The fluorescent intensity in the shapes varies because of the inhomogeneous distribution of the stress.

It is well known that the DIW printing method could be employed to print the structure with multiple materials by simply switching the extrusion reservoir. The mechanochromic behavior of the DNHs is highly dependent on the concentration of the mechanophores.[46] We explore the fabrication of the hydrogel structures which are capable of multi-color change in desired patterns with microgel printing inks containing different mechanophore concentrations. The microgel printing inks are prepared with different concentrations of HPR mechanophores, which are 0, 1, and 2 mol % relative to the concentration of the monomer AMPS in the first network. The total amount of the cross-linkers HPR mechanophore and MBAA are the same as 4 mol % in the PAMPS network. We first print the hydrogels in a rectangular shape with these microgel inks. The printed hydrogels are

https://doi.org/10.1021/acsami.2c22564
ACS Appl. Mater. Interfaces 2023, 15, 11122−11130

cured under a flood irradiation of UV light (365 nm) for 15 min. Then, we stretch the printed rectangular hydrogel structures and record the fluorescent spectra (Figures S7 and S8). Figure 3e shows the relationship between the normalized fluorescent intensity at 566 nm versus the stretch. The printed hydrogel with 2 mol % HPR mechanophores has a larger increase compared with that with 1 mol % HPR mechanophores. The difference in the color change enables us to fabricate a mechanochromic hydrogel structure with desired fluorescent patterns by the multi-material microgel 3D printing technique. As shown in Figure 3f, the as-printed structure with multiple microgel inks is transparent and colorless. There are no obvious boundaries observed between the different parts of the hydrogels in the ambient light. The tensile test result is comparable with that of the DNHs printed with single microgel ink. The hydrogel does not break at the interface, indicating that the bonding between different hydrogel parts remains strong (Figure S9). The newly formed PAAm network could combine different hydrogel parts together through the topological adhesion effect, which has been reported previously.[51] When the stretch reaches 2, the printed hydrogel shows a colored pattern with colorless, reddish, and red in different parts. Under the irradiation of UV light, the middle part and right part of the printed hydrogel demonstrate fluorescent yellow green and orange colors upon stretching. The multi-material printing technique provides a powerful method to construct the desired mechanochromic patterns.

Compared with tailoring the concentration of the mechanophores, preparing the microgel inks with different mechanophores would lead to a color change with high contrast. Thus, we make the printing inks with the mechanophore triacrylic ester of rhodamine (TAR). The TAR mechanophore is synthesized following the procedures reported previously.[18] It is a three-armed cross-linker, containing three acrylate groups in each molecule. The mechanophore TAR has a distinct rhodamine backbone from the HPR mechanophore and shows a reddish fluorescent color upon mechanical stretching. We prepare the microgel ink containing TAR mechanophores using similar procedures to the HPR mechanophore-contained microgel ink. The rheological behaviors of the TAR-based microgel inks with a microgel concentration of 30, 40, and 50 mg/mL are studied by the flow and oscillation sweep modes at room temperature (Figure S10). With the same concentration, the viscosity of the microgel inks containing TAR mechanophores is higher than that containing HPR mechanophores. It is because the TAR mechanophore has three acrylate groups and the cross-linking density of the corresponding microgel is a little larger. It is found that the microgel ink with a concentration of 50 mg/mL would block the nozzle, while that with a concentration of 30 mg/mL could not maintain the filament shape after extrusion. Thus, we prepare the TAR-embedded microgel ink with a concentration of 40 mg/mL in the following printing experiments.

The hydrogel printed with the microgel ink containing TAR mechanophores exhibits a strength of 0.67 MPa and a strain at breakage of 149% (Figure S11). After stretching, the printed hydrogel with TAR mechanophores changes from colorless to purple in the ambient light and emits a bright fluorescent reddish color with a fluorescent emission wavelength of 605 nm (Figure 4a,b). The color goes deeper as the stretch increases. We plot the relationship between the fluorescent intensity at 605 nm and the stretch in Figure S12. The result shows that when the strain reaches 40%, the hydrogel shows a significant increase in the fluorescent intensity at 605 nm, while the stress is as low as 75 kPa. The difference between the optical properties of the printed hydrogels containing TAR and HPR mechanophores enables us to fabricate the desired color change patterns through the microgel printing method.

We further explore printing a hydrogel sheet with three different kinds of microgel inks, which contain no mechanophore, HPR mechanophores, and TAR mechanophores (Figure 4c). The printed hydrogel is colorless under the ambient light and displays the multi-color pattern with colorless, orange, and purple from left to right, after stretching. Under the irradiation of the UV light, the middle part and right part of stretched hydrogel sample emit fluorescent yellow and orange color, respectively. We print a star shape with three kinds of microgel inks which contain no mechanophore, HPR mechanophores, and TAR mechanophores (Figure 4d). The printed hydrogel shape demonstrates a colored pattern after compression. The result shows that the microgel printing method could be effective in constructing the mechanochromic patterns in arbitrary shapes. Then, we print an octopus hydrogel structure with the microgel ink containing HPR and TAR mechanophores (Figure 4e). The printed hydrogel octopus shows a good camouflage effect in the sandy substrate. After compression, the octopus changes into a red color, which is easily found in the sands. The capability of fabricating the color-change patterns provides great potential in the camouflage and signal communications.

3. CONCLUSIONS

In conclusion, we report a multi-material 3D printing method to fabricate mechanochromic hydrogels with desired patterns and shapes. We first covalently incorporate the mechanophores into the first network hydrogel and prepare the microparticles by freeze-drying and grinding. The microparticles are swollen in the second network precursor to prepare a microgel ink. The rheological behaviors of the microgel ink are well-studied, and the printing parameters are optimized. After extrusion, the mechanochromic hydrogel structures are cured under UV light. The printed hydrogels exhibit typical mechanochromic behavior when stretched or compressed. We further demonstrate that the mechanochromic patterned hydrogels could be fabricated through the multi-material printing technique by either adjusting the concentration of the mechanophore or incorporating different mechanophores in the microgel inks. The mechanochromic materials have shown great potential in the camouflage,[52] signal communication,[53] and mechanical failure detection[54,55] through the color change ability. We believe that our work will open an avenue for the fabrication of the mechanochromic device with arbitrary patterns and shapes in the future.

4. EXPERIMENTAL SECTION

4.1. Materials. 2-Acrylamido-2-methyl-1-propanesulfonic acid (AMPS, 98%, Innochem), acrylamide (AAm, 99%, Innochem), *N*,*N*′-methylenebisacrylamide (MBAA, 99%, Innochem), *N*,*N*,*N*′,*N*′-tetramethylethylenediamine (TEMED, 99%, Innochem), ammonium persulfate (APS, Aladdin), and 2-hydroxy-4′-(2-hydroxyethoxy)-2-methylpropiophenone (I2959, 98%, Innochem) were used as received. All the solvents were used as received without further purification.

https://doi.org/10.1021/acsami.2c22564
ACS Appl. Mater. Interfaces 2023, 15, 11122−11130

4.2. Characterization. The grain size distribution of the PAMPS microparticles is measured using a laser particle analyzer (Malvern, Mastersize 3000). The rheological properties of the hydrogel inks are measured using a rheometer (Discovery, DHR-2). The G' and G'' of the ink are measured by the oscillatory stress sweep method in the range of 0.1−1000 Pa. The viscosity of the ink is measured with a continuously ramped shear rate (from 0.1 to 100 s^{-1}). Uniaxial tensile tests of the hydrogels are carried out on a universal material testing machine (Ulm-Einsingen, Zwick) with a 500 N load cell. The hydrogel samples are cut into a rectangular shape with a size of 10 mm × 30 mm × 1 mm. During the uniaxial tensile test, the strain rate is kept at 0.5 min^{-1}. The fluorescence measurements are performed on the fluorescence spectrometer (Hitachi, F-7000). The excitation wavelength is set as 365 nm. The scanning speed is 1200 nm/min. The fluorescent spectra are recorded from 375 to 720 nm. The optical images are taken by a NIKON Z5 camera.

4.3. Synthesis of Mechanophores. The HPR and TAR mechanophores are synthesized following the procedures reported previously (Schemes S1 and S2).[18,46] The chemical structures of the synthesized compounds are verified by ^{1}H NMR and high-resolution mass spectroscopy, as shown in the Supporting Information.

4.4. Preparation of PAMPS Microparticles. The monomer AMPS (2.31 g, 10 mmol), the cross-linker MBAA (0.031 g, 0.2 mmol), and the thermal initiator APS (0.045 g, 0.2 mmol) were dissolved in 9 mL of water. Then, a solution of the cross-linker HPR mechanophore (0.11 g, 0.2 mmol) in DMSO (1 mL) was added. After that, the catalyst TEMED (0.15 mL, 1 mmol) was slowly added to the mixture dropwise. The mixture was poured into a glass mold with a height of 3 mm and cured at 50 °C for 1 h. The obtained PAMPS hydrogel was immersed in sodium hydroxide solution (1×10^{-2} mol/L) overnight. After that, the PAMPS hydrogel was pre-frozen with liquid nitrogen for 15 min and then freeze-dried. The freeze-dried PAMPS network is ground using ball milling (245 rpm). The ground powders are collected after passing through the sieve with a size of 150 μm. The microparticles with TAR mechanophores are prepared in similar procedures with MBAA (0.015 g, 0.1 mmol) and TAR (0.14 g, 0.2 mmol) as the cross-linkers.

4.5. Preparation of the Microgel Printing Inks. The second network monomer AAm (1.42 g, 20 mmol), the photoinitiator I2959 (0.0225 g, 0.1 mmol), and the cross-linker MBAA (0.0003 g, 0.002 mmol) were dissolved in borax/sodium hydroxide buffer solution (pH = 10, 5 mL). Then, 0.25 g of PAMPS microparticles is added to 5 mL of the precursor solution to produce the microgel printing ink. The ink was stored at 2−8 °C for 12 h. After 3D printing, the printed hydrogel structures are cured under a flood irradiation of UV light (365 nm) for 15 min. The inks with TAR mechanophores are prepared in the similar procedures.

■ ASSOCIATED CONTENT

Supporting Information

The Supporting Information is available free of charge at https://pubs.acs.org/doi/10.1021/acsami.2c22564.

Synthetic route of HPR and TAR mechanophores, photograph of microparticles and microgel inks, size characterization of the microparticles, results of mechanical tests, rheology tests, and fluorescence spectra (PDF)

■ AUTHOR INFORMATION

Corresponding Author

Zhijian Wang − *Key Laboratory of Aerospace Advanced Materials and Performance, Ministry of Education, School of Materials Science and Engineering, Beihang University, Beijing 100191, China;* orcid.org/0000-0003-2929-8376; Email: zhijianw@buaa.edu.cn

Authors

Bo Xu − *Key Laboratory of Aerospace Advanced Materials and Performance, Ministry of Education, School of Materials Science and Engineering, Beihang University, Beijing 100191, China*

Hezhen Wang − *Key Laboratory of Aerospace Advanced Materials and Performance, Ministry of Education, School of Materials Science and Engineering, Beihang University, Beijing 100191, China*

Zixiong Luo − *Key Laboratory of Aerospace Advanced Materials and Performance, Ministry of Education, School of Materials Science and Engineering, Beihang University, Beijing 100191, China*

Jiping Yang − *Key Laboratory of Aerospace Advanced Materials and Performance, Ministry of Education, School of Materials Science and Engineering, Beihang University, Beijing 100191, China;* orcid.org/0000-0001-7207-0233

Complete contact information is available at: https://pubs.acs.org/10.1021/acsami.2c22564

Author Contributions

B.X. and Z.W. conceived the ideas and designed the research. B.X., H.W., and Z.L. carried out the experiments. B.X. drafted the manuscript. Z.W. and J.Y. revised the manuscript. The final manuscript was written through contributions of all authors.

Notes

The authors declare no competing financial interest.

■ ACKNOWLEDGMENTS

Z.W. greatly acknowledges the financial support by the Beijing Natural Science Foundation (2222058), the National Natural Science Foundation of China (52105003), and the Fundamental Research Funds for the Central Universities (YWF-22-K-101).

■ REFERENCES

(1) Wilson, D. J.; Lin, Z.; Bower, D. Q.; Deravi, L. F. Engineering Color, Pattern, and Texture: From Nature to Materials. *Matter* **2021**, *4*, 2163−2171.

(2) Zeng, S.; Zhang, D.; Huang, W.; Wang, Z.; Freire, S. G.; Yu, X.; Smith, A. T.; Huang, E. Y.; Nguon, H.; Sun, L. Bio-inspired Sensitive and Reversible Mechanochromisms via Strain-dependent Cracks and Folds. *Nat. Commun.* **2016**, *7*, 11802.

(3) Wang, Z.; Fan, W.; He, Q.; Wang, Y.; Liang, X.; Cai, S. A Simple and Robust Way towards Reversible Mechanochromism: Using Liquid Crystal Elastomer as a Mask. *Extreme Mech. Lett.* **2017**, *11*, 42−48.

(4) Li, C.; He, Q.; Wang, Y.; Wang, Z.; Wang, Z.; Annapooranan, R.; Latz, M. I.; Cai, S. Highly Robust and Soft Biohybrid Mechanoluminescence for Optical Signaling and Illumination. *Nat. Commun.* **2022**, *13*, 3914.

(5) Morin, S. A.; Shepherd, R. F.; Kwok, S. W.; Stokes, A. A.; Nemiroski, A.; Whitesides, G. M. Camouflage and Display for Soft Machines. *Science* **2012**, *337*, 828−832.

(6) Chen, G.; Hong, W. Mechanochromism of Structural-Colored Materials. *Adv. Opt. Mater.* **2020**, *8*, 2000984.

(7) Clough, J. M.; Weder, C.; Schrettl, S. Mechanochromism in Structurally Colored Polymeric Materials. *Macromol. Rapid Commun.* **2021**, *42*, No. e2000528.

(8) Pucci, A.; Ruggeri, G. Mechanochromic Polymer Blends. *J. Mater. Chem.* **2011**, *21*, 8282−8291.

(9) Han, T.; Liu, L.; Wang, D.; Yang, J.; Tang, B. Mechanochromic Fluorescent Polymers Enabled by AIE Processes. *Macromol. Rapid Commun.* **2021**, *42*, No. e2000311.

(10) Kim, D.; Kwon, M. S.; Lee, C. W. Mechanochromic Polymers with a Multimodal Chromic Transition: Mechanophore Design and Transduction Mechanism. *Polym. Chem.* **2022**, *13*, 5177−5187.
(11) Chen, Y.; Mellot, G.; van Luijk, D. V.; Creton, C.; Sijbesma, R. P. Mechanochemical Tools for Polymer Materials. *Chem. Soc. Rev.* **2021**, *50*, 4100−4140.
(12) Ghanem, M. A.; Basu, A.; Behrou, R.; Boechler, N.; Boydston, A. J.; Craig, S. L.; Lin, Y.; Lynde, B. E.; Nelson, A.; Shen, H.; Storti, D. W. The Role of Polymer Mechanochemistry in Responsive Materials and Additive Manufacturing. *Nat. Rev. Mater.* **2020**, *6*, 84−98.
(13) Davis, D. A.; Hamilton, A.; Yang, J.; Cremar, L. D.; Van Gough, D.; Potisek, S. L.; Ong, M. T.; Braun, P. V.; Martínez, T. J.; White, S. R.; Moore, J. S.; Sottos, N. R. Force-Induced Activation of Covalent Bonds in Mechanoresponsive Polymeric Materials. *Nature* **2009**, *459*, 68−72.
(14) Kim, T. A.; Robb, M. J.; Moore, J. S.; White, S. R.; Sottos, N. R. Mechanical Reactivity of Two Different Spiropyran Mechanophores in Polydimethylsiloxane. *Macromolecules* **2018**, *51*, 9177−9183.
(15) Lee, C. K.; Beiermann, B. A.; Silberstein, M. N.; Wang, J.; Moore, J. S.; Sottos, N. R.; Braun, P. V. Exploiting Force Sensitive Spiropyrans as Molecular Level Probes. *Macromolecules* **2013**, *46*, 3746−3752.
(16) Zhang, H.; Chen, Y.; Lin, Y.; Fang, X.; Xu, Y.; Ruan, Y.; Weng, W. Spiropyran as a Mechanochromic Probe in Dual Cross-Linked Elastomers. *Macromolecules* **2014**, *47*, 6783−6790.
(17) Wang, Z.; Ma, Z.; Wang, Y.; Xu, Z.; Luo, Y.; Wei, Y.; Jia, X. A Novel Mechanochromic and Photochromic Polymer Film: When Rhodamine Joins Polyurethane. *Adv. Mater.* **2015**, *27*, 6469−6474.
(18) Wang, T.; Zhang, N.; Dai, J.; Li, Z.; Bai, W.; Bai, R. Novel Reversible Mechanochromic Elastomer with High Sensitivity: Bond Scission and Bending-Induced Multicolor Switching. *ACS Appl. Mater. Interfaces* **2017**, *9*, 11874−11881.
(19) Wu, C.; Tu, C.; Aimi, J.; Zhang, J.; Chen, T.; Wang, C.; Huang, C. Mechanochromic Double Network Hydrogels as a Compression Stress Sensor. *Polym. Chem.* **2020**, *11*, 6423−6428.
(20) Yang, F.; Li, X.; Chen, Y. A Chromic and Near-Infrared Emissive Mechanophore Serving as a Versatile Force Meter in Micelle-Hydrogel Composites. *Adv. Opt. Mater.* **2022**, *10*, 2102552.
(21) Chen, Y.; Spiering, A. J.; Karthikeyan, S.; Peters, G. W.; Meijer, E. W.; Sijbesma, R. P. Mechanically Induced Chemiluminescence from Polymers Incorporating a 1,2-Dioxetane Unit in the Main Chain. *Nat. Chem.* **2012**, *4*, 559−562.
(22) Chen, W.; Yuan, Y.; Chen, Y. Visualized Bond Scission in Mechanochemiluminescent Polymethyl Acrylate/Cellulose Nanocrystals Composites. *ACS Macro Lett.* **2020**, *9*, 438−442.
(23) Li, X.; Li, J.; Wei, W.; Yang, F.; Wu, M.; Wu, Q.; Xie, T.; Chen, Y. Enhanced Mechanochemiluminescence from End-Functionalized Polyurethanes with Multiple Hydrogen Bonds. *Macromolecules* **2021**, *54*, 1557−1563.
(24) Imato, K.; Irie, A.; Kosuge, T.; Ohishi, T.; Nishihara, M.; Takahara, A.; Otsuka, H. Mechanophores with a Reversible Radical System and Freezing-induced Mechanochemistry in Polymer Solutions and Gels. *Angew. Chem., Int. Ed.* **2015**, *54*, 6168−6172.
(25) Oka, H.; Imato, K.; Sato, T.; Ohishi, T.; Goseki, R.; Otsuka, H. Enhancing Mechanochemical Activation in the Bulk State by Designing Polymer Architectures. *ACS Macro Lett.* **2016**, *5*, 1124−1127.
(26) Imato, K.; Natterodt, J. C.; Sapkota, J.; Goseki, R.; Weder, C.; Takahara, A.; Otsuka, H. Dynamic Covalent Diarylbibenzofuranone-modified Nanocellulose: Mechanochromic Behaviour and Application in Self-healing Polymer Composites. *Polym. Chem.* **2017**, *8*, 2115−2122.
(27) Göstl, R.; Sijbesma, R. P. π-Extended Anthracenes as Sensitive Probes for Mechanical Stress. *Chem. Sci.* **2016**, *7*, 370−375.
(28) Hu, X.; Zeng, T.; Husic, C. C.; Robb, M. J. Mechanically Triggered Release of Functionally Diverse Molecular Payloads from Masked 2-Furylcarbinol Derivatives. *ACS Cent. Sci.* **2021**, *7*, 1216−1224.
(29) Wang, Q.; Gossweiler, G. R.; Craig, S. L.; Zhao, X. Cephalopod-Inspired Design of Electro-Mechano-Chemically Responsive Elastomers for on-demand Fluorescent Patterning. *Nat. Commun.* **2014**, *5*, 4899.
(30) Peterson, G. I.; Larsen, M. B.; Ganter, M. A.; Storti, D. W.; Boydston, A. J. 3D-Printed Mechanochromic Materials. *ACS Appl. Mater. Interfaces* **2015**, *7*, 577−583.
(31) Rohde, R. C.; Basu, A.; Okello, L. B.; Barbee, M. H.; Zhang, Y.; Velev, O. D.; Nelson, A.; Craig, S. L. Mechanochromic Composite Elastomers for Additive Manufacturing and Low Strain Mechanophore Activation. *Polym. Chem.* **2019**, *10*, 5985−5991.
(32) Yao, M.; Wei, Z.; Li, J.; Guo, Z.; Yan, Z.; Sun, X.; Yu, Q.; Wu, X.; Yu, C.; Yao, F.; Feng, S.; Zhang, H.; Li, J. Microgel Reinforced Zwitterionic Hydrogel Coating for Blood-Contacting Biomedical Devices. *Nat. commun.* **2022**, *13*, 5339.
(33) Daly, A. C.; Riley, L.; Segura, T.; Burdick, J. A. Hydrogel Microparticles for Biomedical Applications. *Nat. Rev. Mater.* **2020**, *5*, 20−43.
(34) Yuk, H.; Lu, B.; Zhao, X. Hydrogel Bioelectronics. *Chem. Soc. Rev.* **2019**, *48*, 1642−1667.
(35) Luo, J.; Yang, J.; Zheng, X.; Ke, X.; Chen, Y.; Tan, H.; Li, J. A Highly Stretchable, Real-Time Self-Healable Hydrogel Adhesive Matrix for Tissue Patches and Flexible Electronics. *Adv. Healthc. Mater.* **2020**, *9*, 1901423.
(36) Hu, L.; Chee, P. L.; Sugiarto, S.; Yu, Y.; Shi, C.; Yan, R.; Yao, Z.; Shi, X.; Zhi, J.; Kai, D.; Yu, H.-D.; Huang, W. Hydrogel-Based Flexible Electronics. *Adv. Mater.* **2022**, *34*, 2205326.
(37) Lin, S.; Yuk, H.; Zhang, T.; Parada, G. A.; Koo, H.; Yu, C.; Zhao, X. Stretchable Hydrogel Electronics and Devices. *Adv. Mater.* **2016**, *28*, 4497−4505.
(38) Shen, Z.; Zhang, Z.; Zhang, N.; Li, J.; Zhou, P.; Hu, F.; Rong, Y.; Lu, B.; Gu, G. High-Stretchability, Ultralow-Hysteresis Conducting Polymer Hydrogel Strain Sensors for Soft Machines. *Adv. Mater.* **2022**, *34*, 2203650.
(39) Wirthl, D.; Pichler, R.; Drack, M.; Kettlguber, G.; Moser, R.; Gerstmayr, R.; Hartmann, F.; Bradt, E.; Kaltseis, R.; Siket, C. M.; Schausberger, S. E.; Hild, S.; Bauer, S.; Kaltenbrunner, M. Instant Tough Bonding of Hydrogels for Soft Machines and Electronics. *Sci. Adv.* **2017**, *3*, No. e1700053.
(40) Wei, S.; Lu, W.; Le, X.; Ma, C.; Lin, H.; Wu, B.; Zhang, J.; Theato, P.; Chen, T. Bioinspired Synergistic Fluorescence-Color-Switchable Polymeric Hydrogel Actuators. *Angew. Chem.* **2019**, *131*, 16389−16397.
(41) Yuk, H.; Wu, J.; Zhao, X. Hydrogel Interfaces for Merging Humans and Machines. *Nat. Rev. Mater.* **2022**, *7*, 935−952.
(42) Zhao, Y.; Lo, C. Y.; Ruan, L.; Pi, C. H.; Kim, C.; Alsaid, Y.; Frenkel, I.; Rico, R.; Tsao, T. C.; He, X. Somatosensory Actuator Based on Stretchable Conductive Photothermally Responsive Hydrogel. *Sci. Robot.* **2021**, *6*, No. eabd5483.
(43) Yuk, H.; Lin, S.; Ma, C.; Takaffoli, M.; Fang, N. X.; Zhao, X. Hydraulic Hydrogel Actuators and Robots Optically and Sonically Camouflaged in Water. *Nat. Commun.* **2017**, *8*, 14230.
(44) Chen, Y.; Li, Q.; Wang, Q.; Yuan, Y. Mechanochemiluminescent Hydrogels for Real-Time Visualization of Chemical Bond Scission. *Synlett* **2022**, *33*, 879−884.
(45) Chen, H.; Yang, F.; Chen, Q.; Zheng, J. A Novel Design of Multi-Mechanoresponsive and Mechanically Strong Hydrogels. *Adv. Mater.* **2017**, *29*, 1606900.
(46) Xu, B.; Luo, Z.; Xiao, R.; Wang, Z.; Yang, J. Hybrid Phenol-Rhodamine Dye Based Mechanochromic Double Network Hydrogels with Tunable Stress Sensitivity. *Macromol. Rapid Commun.* **2022**, *43*, 2200580.
(47) Zhao, D.; Liu, Y.; Liu, B.; Chen, Z.; Nian, G.; Qu, S.; Yang, W. 3D Printing Method for Tough Multifunctional Particle-Based Double-Network Hydrogels. *ACS Appl. Mater. Interfaces* **2021**, *13*, 13714−13723.
(48) Hirsch, M.; Charlet, A.; Amstad, E. 3D Printing of Strong and Tough Double Network Granular Hydrogels. *Adv.Funct. Mater.* **2020**, *31*, 2005929.

https://doi.org/10.1021/acsami.2c22564
ACS Appl. Mater. Interfaces 2023, 15, 11122−11130

(49) Highley, C. B.; Song, K. H.; Daly, A. C.; Burdick, J. A. Jammed Microgel Inks for 3D Printing Applications. *Adv. Sci.* **2019**, *6*, 1801076.
(50) Kessler, M.; Nassisi, Q.; Amstad, E. Does the Size of Microgels Influence the Toughness of Microgel-Reinforced Hydrogels? *Macromol. Rapid Commun.* **2022**, *43*, No. e2200196.
(51) Yang, J.; Bai, R.; Chen, B.; Suo, Z. Hydrogel Adhesion: A Supramolecular Synergy of Chemistry, Topology, and Mechanics. *Adv. Funct. Mater.* **2020**, *30*, 1901693.
(52) Gossweiler, G. R.; Brown, C. L.; Hewage, G. B.; Sapiro-Gheiler, E.; Trautman, W. J.; Welshofer, G. W.; Craig, S. L. Mechanochemically Active Soft Robots. *ACS Appl. Mater. Interfaces* **2015**, *7*, 22431−22435.
(53) Giordano, G.; Gagliardi, M.; Huan, Y.; Carlotti, M.; Mariani, A.; Menciassi, A.; Sinibaldi, E.; Mazzolai, B. Toward Mechanochromic Soft Material-Based Visual Feedback for Electronics-Free Surgical Effectors. *Adv. Sci.* **2021**, *8*, 2100418.
(54) Chen, Y.; Yeh, C. J.; Qi, Y.; Long, R.; Creton, C. From Force-Responsive Molecules to Quantifying and Mapping Stresses in Soft Materials. *Sci. Adv.* **2020**, *6*, No. eaaz5093.
(55) Deneke, N.; Rencheck, M. L.; Davis, C. S. An Engineer's Introduction to Mechanophores. *Soft Matter* **2020**, *16*, 6230−6252.

Recommended by ACS

Trifunctional Microgel-Mediated Preparation and Toughening of Printable High-Performance Chitosan Hydrogels for Underwater Communications

Baokang Wang, You Yu, *et al.*

FEBRUARY 08, 2023
ACS APPLIED MATERIALS & INTERFACES

READ

Tough, Healable, and Sensitive Strain Sensor Based on Multiphysically Cross-Linked Hydrogel for Ionic Skin

Yue Xin, Xin He, *et al.*

FEBRUARY 06, 2023
BIOMACROMOLECULES

READ

Frontal Polymerization and Three-Dimensional Printing of Thermoset Polymers with Tunable Thermomechanical Properties

Morteza Ziaee, Mostafa Yourdkhani, *et al.*

FEBRUARY 13, 2023
ACS APPLIED POLYMER MATERIALS

READ

Analysis of Poly(thiourethane) Covalent Adaptable Network through Broadband Dielectric Spectroscopy

B. Pascual-Jose, A. Ribes-Greus, *et al.*

JANUARY 06, 2023
ACS APPLIED POLYMER MATERIALS

READ

Get More Suggestions >

https://doi.org/10.1021/acsami.2c22564
ACS Appl. Mater. Interfaces 2023, 15, 11122−11130